

# The Magnetic Field, Temperature and Strain Dependence of the Critical Current of a Nb<sub>3</sub>Sn Strand Using a Six Free-Parameter Scaling Law

XiFeng Lu and Damian P. Hampshire

**Abstract**—We report comprehensive data for the magnetic field ( $B < 14.5$  T), temperature ( $4.2 \text{ K} \leq T \leq 14 \text{ K}$ ) and uniaxial applied strain dependence ( $-1\% < \varepsilon_A < 0.35\%$ ) of the critical current density ( $J_C$ ) of an advanced internal-tin Nb<sub>3</sub>Sn strand developed as part of the International Thermonuclear Experimental Reactor (ITER) program manufactured by Luvata PORI. A very short heat-treatment was used so that  $J_C$  of the PORI Nb<sub>3</sub>Sn strand was  $\sim 40\%$  lower than optimized values. Despite the low  $J_C$ , we find that the normalized strain sensitivity of the critical current at 14 T and 4.2 K is similar to other advanced internal-tin Nb<sub>3</sub>Sn strands. By assuming that the strain dependence of the normalized effective upper critical field is similar to that specified for other advanced strands, the  $J_C(B, T, \varepsilon)$  data of the PORI strand can be accurately parameterized using a scaling law with just 6 free parameters. Hence the results presented here on a low  $J_C$  strand provide evidence that the 6 free parameter scaling law can be expected to accurately characterize a wide range of advanced internal-tin Nb<sub>3</sub>Sn strands. The index of transition or  $n$  value is described by a modified power law of the form  $n = 1 + rI_C^s$ , where  $r$  and  $s$  are approximately constant with values 3.15 and 0.36 respectively.

**Index Terms**—Critical current density, Nb<sub>3</sub>Sn strand, scaling law, uniaxial strain.

## I. INTRODUCTION

THERE HAS BEEN the very fast development of Nb<sub>3</sub>Sn strands in the last decade due to the requirement for large superconducting magnets—particularly motivated by the International Thermonuclear Experimental Reactor (ITER) project [1], [2]. The improvement has been focused on increasing the critical current density ( $J_C$ ) and decreasing the cost [3]. With high critical current density (non-Cu  $J_C$  800–1200 A · mm<sup>-2</sup> at 4.2 K and 12 T) and acceptable ac losses ( $\sim 600 \text{ kJ} \cdot \text{m}^{-3}$ ), the use of advanced internal-tin Nb<sub>3</sub>Sn strands is very attractive. As a result, significant effort has transferred from producing bronze-route strands (where non-Cu  $J_C < 800 \text{ A} \cdot \text{mm}^{-2}$ ) to advanced internal-tin strands. The  $J_C$  (and  $I_C$ ) versus magnetic field with zero applied strain of these two types of strands are shown in Fig. 1. The differences between the  $J_C$  (and  $I_C$ ) values over a wide field range are clear.

It is well established that the effects of strain on technological Nb<sub>3</sub>Sn strands must be characterized over a wide magnetic

field and temperature range [4]–[11], because large stresses are unavoidable in large magnets originating from the differential thermal contraction between the components of the magnets during the process of cool-down and also the large Lorentz forces produced during high field operation. In this paper we present comprehensive  $J_C(B, T, \varepsilon)$  data as a function of magnetic field ( $B < 14.5$  T), temperature ( $4.2 \text{ K} \leq T \leq 14 \text{ K}$ ) and uniaxial applied strain ( $-1\% < \varepsilon_A < 0.35\%$ ) for an advanced internal-tin PORI Nb<sub>3</sub>Sn strand developed for the ITER project. By using a short heat-treatment,  $J_C$  is significantly reduced from optimum values which allows us to assess whether we can expect the 6 free parameter scaling law recently proposed [12] for advanced internal-tin strands to be of general validity for strands reacted with different heat-treatments.

## II. EXPERIMENTAL PROCEDURE

### A. Sample and Heat Treatment

The PORI strand, of diameter 0.81 mm, investigated in this paper was manufactured by Luvata PORI using sub-elements developed for the KSTAR project [13]. The strand was heat-treated in an argon atmosphere on oxidized stainless-steel mandrels in a three-zone furnace, with an additional thermocouple positioned next to the sample in order to monitor and control the temperature using the heat-treatment: 210°C for 48 h; 400°C for 48 h; 640°C for 60 h (all the ramp rates were 10°C · h<sup>-1</sup>). This heat-treatment time is much shorter and hence the  $I_C$  much lower than that for maximum/optimum values [12]. Nevertheless, the  $I_C$  for the PORI strand is still significantly higher than that of bronze-route (Vac and Furukawa) strands as seen in Fig. 1. After reaction, the wires were etched in hydrochloric acid to remove the chrome and transferred to nickel-plated Ti-6Al-4V helical springs, to which they were attached using copper plating and soldering. An optimized helical spring [14], [15] was used for the  $J_C(B, T, \varepsilon)$  measurements.

### B. Apparatus and Techniques

After the PORI strand was attached to the spring, it was mounted onto our purpose-built  $J_C(B, T, \varepsilon)$  probe [7], [10], [16]. The critical current measurements were carried out in Durham in magnetic fields up to 14.5 Tesla. Throughout this paper, the engineering  $J_C$  is quoted, which is defined as  $I_C$  divided by the entire cross-sectional area of the strand. For variable strain measurements, the spring is twisted to apply the strain to the wire via a worm-and-wheel system. For variable-temperature measurements above 4.2 K, the probe

Manuscript received August 15, 2008. First published June 30, 2009; current version published July 15, 2009. This work was supported by EFDA and EPSRC.

The authors are with the Superconductivity Group, Department of Physics, University of Durham, Durham DH1 3LE, U.K. (e-mail: d.p.hampshire@durham.ac.uk; xifeng.lu@durham.ac.uk).

Digital Object Identifier 10.1109/TASC.2009.2018847

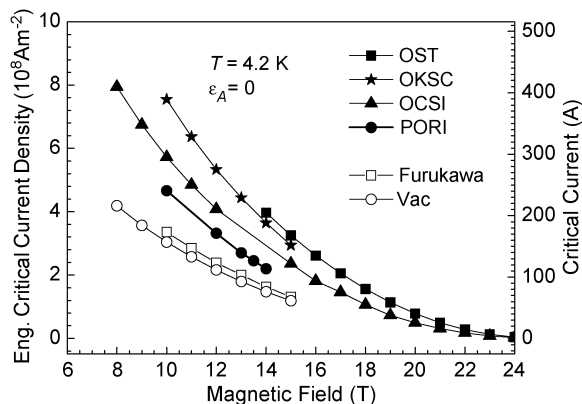


Fig. 1. Engineering critical current density  $J_C$  (and critical current  $I_C$ ) versus magnetic field for  $\text{Nb}_3\text{Sn}$  strands made by different manufacturers. The Vac (now known as EAS) and Furukawa strands are bronze-route. OST, OKSC, OCSI and PORI strands are advanced internal-tin.

provides a vacuum chamber around the sample and the temperature is maintained during the measurement using three sets of independently controlled Cernox thermometers and constantan wire heaters distributed to produce a uniform temperature profile along the turns of the spring. For measurements at 4.2 K, the sample is in direct contact with the liquid helium.

At specified values of magnetic field, temperature and strain, measurements are made of the voltage ( $V$ ) across sections of the strand as a function of the current through it. The voltage noise is typically a few nV predominantly due to the Johnson noise from the voltage leads. The voltage across a section of the wire was measured using a nanovolt amplifier and a digital voltmeter and the current was measured using a four-terminal standard resistor. The electric field criterion used for  $J_C$  is  $10 \mu\text{V} \cdot \text{m}^{-1}$  and the index of transition or  $n$ -value is calculated using the power-law expression  $E \propto J^n$  with  $E$  in the range between 10 and  $100 \mu\text{V} \cdot \text{m}^{-1}$ . Details of the experimental apparatus and techniques have been provided previously [15], [17], [18].

### III. RESULTS

Fig. 2 shows  $J_C$  (and  $I_C$ ) as a function of applied strain at 4.2 K in magnetic fields from 10 T to 14 T with the increment in field of 0.5 T. The well-known inverted quasi-parabolic behavior for  $J_C$  as a function of strain is very clear and the critical role of strain can be seen from noting that  $\pm 0.5\%$  strain (around 4.2 K and 12 T) can decrease  $J_C$  by  $\sim 50\%$ . Fig. 3 provides a comparison between the normalized strain dependence of the critical current for the PORI strand investigated in this work and other optimized advanced internal-tin strands (OST, OKSC and OCSI) reported in the literature [12]. It can be seen that although the magnitude of  $I_C$  is significantly different for each of these four strands, to within the accuracy of the measurements, the strain dependence is very similar.

The  $\text{Nb}_3\text{Sn}$  Cable-In-Conduit-Conductors (CICC) used for the ITER magnet systems operate in supercritical helium at temperatures above 4.2 K. Fig. 4 shows  $J_C$  (and  $I_C$ ) as a function

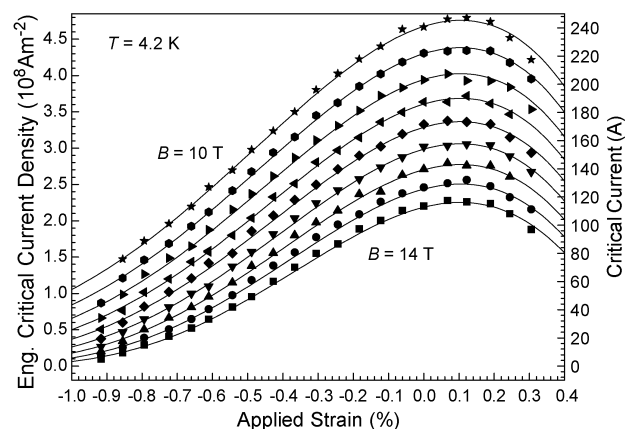


Fig. 2. Engineering critical current density (and critical current) of PORI strand as a function of applied strain at 4.2 K in magnetic fields from 10 and 14 T with increments ( $\Delta B$ ) 0.5 T. The solid lines are provided by the Durham scaling law (with 6 free parameters).

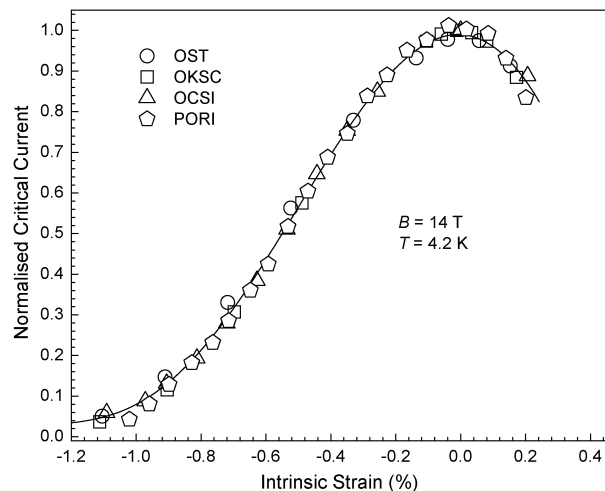


Fig. 3. The normalized critical current at 4.2 K as a function of intrinsic strain for OST ( $I_{\text{Max}} = 219.6$  A), OKSC ( $I_{\text{Max}} = 193.4$  A), OCSI ( $I_{\text{Max}} = 149.6$  A) (taken from [12]), and the PORI ( $I_{\text{Max}} = 116.1$  A) strand reported in this work. The solid line is a guide to the eye.

of applied strain from 6 K to 12 K in different magnetic fields. Limited 14 K data were also measured (not displayed here). The strong magnetic field, temperature and strain dependence of  $J_C$  (and  $I_C$ ) is clearly observed in Figs. 1–4. In Figs. 2 and 4, the data points are the experimental measurements, and the solid lines are provided by the Durham scaling law with 6 free parameters which are provided in Table I. The details of the scaling law will be discussed in the Section IV.

The  $E$ – $J$  characteristics of the superconducting strands were characterized using the power law expression [19]–[21]  $E \propto J^n$ . The  $n$ -value characterizes the sharpness of the  $E$ – $J$  transition in technological superconductors [21]–[24]. The  $n$ -values for the PORI strand were obtained from  $E$ – $J$  characteristics over the technological range of interest from 10 to  $100 \mu\text{V} \cdot \text{m}^{-1}$  and are presented as a function of critical current at different magnetic fields, temperatures and strains in Fig. 5.

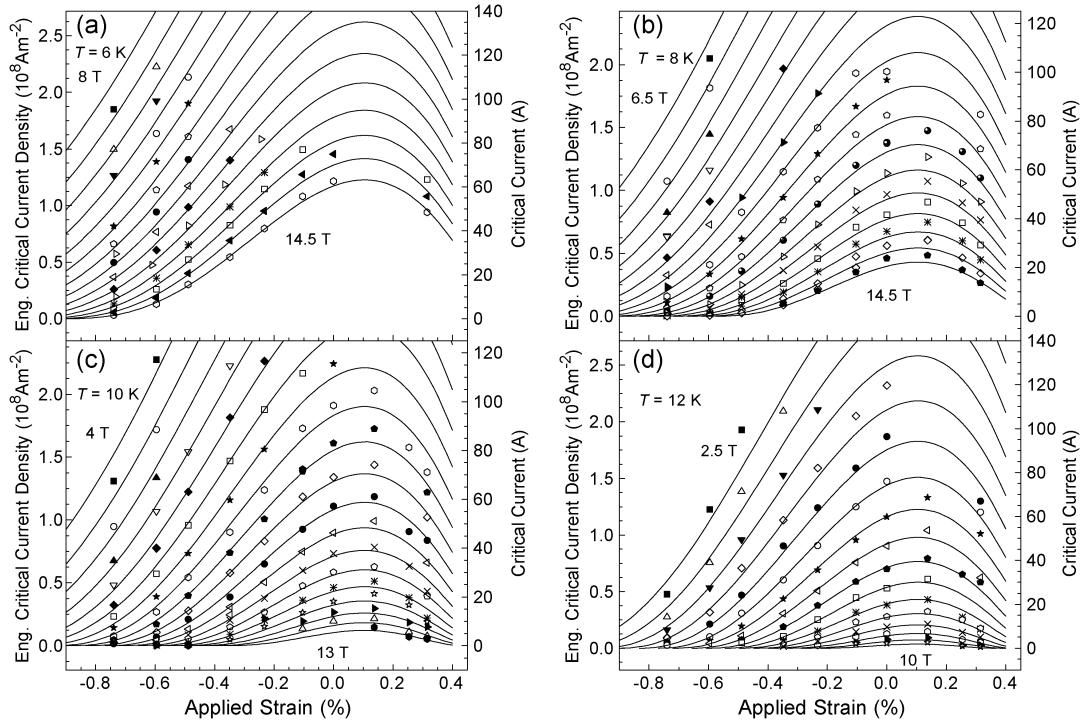


Fig. 4. Engineering critical current density (and critical current) as a function of applied strain at magnetic fields shown. Panels (a)–(d) are at temperatures of 6 K, 8 K, 10 K and 12 K respectively. The lines are provided by the Durham scaling law using (6 free) parameters from Table I.

TABLE I  
PARAMETERS OF DURHAM SCALING LAW FOR PORI STRAND: SIX  
PARAMETERS ARE FREE AND SEVEN, GIVEN IN BOLD, WERE NOT VARIED  
IN THE FITTING PROCEDURE

| Universal Values | $c_2$  | $c_3$           | $c_4$            | $n$           | $\nu$        | $w$                 | $u$      |
|------------------|--|-----------------|------------------|---------------|--------------|---------------------|----------|
|                  | <b>-0.77462</b>                                | <b>-0.59345</b> | <b>-0.13925</b>  | <b>2.5</b>    | <b>1.5</b>   | <b>2.2</b>          | <b>0</b> |
|                  | $A(0)$   | $T_C^*(0)$      | $B_{C_2}^*(0,0)$ | $p$           | $q$          | $\varepsilon_M$ (%) |          |
|                  | ( $\text{Am}^{-2}\text{T}^{-3}\text{K}^{-2}$ ) | (K)             | (T)              |               |              |                     |          |
|                  | <b>3.644</b> $\times 10^7$                     | <b>16.63</b>    | <b>30.01</b>     | <b>1.0129</b> | <b>2.653</b> | <b>0.1044</b>       |          |

#### IV. ANALYSIS

##### A. Variable-Strain Critical Current Data Analysed Using Scaling Laws

Extensive work on a range of different Nb<sub>3</sub>Sn strands fabricated using different manufacturing techniques has lead to a scaling law for  $J_C(B, T, \varepsilon)$  of the form [7]

$$J_C(B, T, \varepsilon_1) = A(\varepsilon_1) [T_C^*(\varepsilon_1)(1 - t^2)]^2 \times [B_{C_2}^*(T, \varepsilon_1)]^{n-3} b^{p-1} (1 - b)^q \quad (1)$$

$$B_{C_2}^*(T, \varepsilon_1) = B_{C_2}^*(0, \varepsilon_1)(1 - t^\nu) \quad (2)$$

$$\left(\frac{A(\varepsilon_1)}{A(0)}\right)^{1/u} = \left(\frac{B_{C_2}^*(0, \varepsilon_1)}{B_{C_2}^*(0, 0)}\right)^{1/w} = \frac{T_C^*(\varepsilon_1)}{T_C^*(0)} \quad (3)$$

where  $J_C$  is the engineering critical current density,  $\varepsilon_A$  is the applied strain,  $\varepsilon_I = \varepsilon_A - \varepsilon_M$  is the intrinsic strain,  $\varepsilon_M$  is the applied strain at the peak in  $J_C$  [25]–[27],  $T_C^*$  is the effective

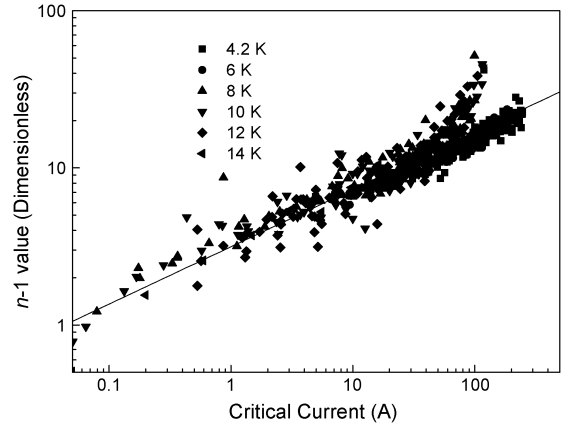


Fig. 5.  $n - 1$  as a function of critical current for PORI strand.

critical temperature,  $t = T/T_C^*$  is the reduced temperature,  $B_{C_2}^*$  is the effective upper critical field and  $b = B/B_{C_2}^*$  is the reduced field. The number of free parameters can be reduced by using universal values for  $n$ ,  $\nu$ ,  $w$  and  $u$  [7], [8].

Recently we reported  $J_C(B, T, \varepsilon)$  measurements made on 3 optimized advanced internal-tin Nb<sub>3</sub>Sn strands in magnetic fields up to 28 Tesla in Grenoble where the upper critical fields were measured directly [12]. Based on those measurements, we proposed a universal strain dependence for the normalized effective upper critical field of advanced strands at  $T = 0$  of the form [12]

$$\frac{B_{C_2}^*(0, \varepsilon_1)}{B_{C_2}^*(0, 0)} = 1 - 0.77462 \cdot \varepsilon_1^2 - 0.59345 \cdot \varepsilon_1^3 - 0.13925 \cdot \varepsilon_1^4 \quad (4)$$

Equations (1)–(4) lead to a  $J_C(B, T, \varepsilon)$  scaling law for advanced internal-tin strands with just six free parameters. The six free parameters for the PORI strand are presented in Table I together

with the other seven parameters that were not varied in the fitting process.

There is good agreement between the experimental  $J_C(B, T, \varepsilon)$  data and the solid lines for the PORI strand shown in Figs. 2 and 4. The data at the lowest reduced fields shows the largest deviation from the scaling law. This is because the reduced field dependence in (1), which includes the parameters  $p$  and  $q$ , is a high-field expression (first proposed in the Fietz-Webb scaling law [28]). It is not sufficiently general to describe the field dependence of over the entire field range. In low fields non-linear terms (in the free-energy [29] and hence required in a pinning description of  $J_C(B, T, \varepsilon)$  [30]) must be included for a more accurate parameterization. Nevertheless, the root-mean-square (RMS) difference between the measured and calculated values of  $I_C$  is about  $\sim 3$  A over the whole measured range. This agreement can be further improved if necessary by using 9 free parameters (not provided here), which gives an RMS difference of  $\sim 2.4$  A.

### B. $n$ -Values

The index of transition or  $n$ -value data are characterized using an empirical modified power law

$$n(B, T, \varepsilon_I) = 1 + r(T, \varepsilon_I) [I_C(B, T, \varepsilon_I)]^{s(T, \varepsilon_I)} \quad (5)$$

As observed previously [20],  $s(T, \varepsilon_I)$  is approximately a constant for all temperatures and applied strains and  $r(T, \varepsilon_I)$  only weakly depends on strain [12], [31]. From Fig. 5 we find that  $r$  and  $s$  are 3.15 and 0.36 respectively, which are values similar to those of other advanced internal-tin strands [12]. We attribute the deviation from linearity at the highest currents in Fig. 5 to heating during the transition.

## V. DISCUSSION

The early development of high  $J_C$  strands for magnet applications involved doping binary  $\text{Nb}_3\text{Sn}$  with elements such as Ta and Ti to increase the upper critical field ( $B_{C2}$ ). Improvements of  $\sim 7$  T were achieved at the expense of a stronger strain dependence for  $B_{C2}$  which can be explained using standard microscopic theory [7]. It follows that strands made using different fabrication routes, which lead to  $\text{Nb}_3\text{Sn}$  with different Sn content will have different reversible strain dependencies—consistent with the differences observed recently between bronze route strands and advanced internal-tin strands [7]. It is well-known that during the heat treatment of strands, the average Sn content and the morphology of the first  $\text{Nb}_3\text{Sn}$  that is formed is quite different to the average properties of the final  $\text{Nb}_3\text{Sn}$  layer [32], [33]. This opens the possibility that even strands fabricated in a similar way may not have a similar strain dependence if the heat-treatment is significantly different. However, in this work we have found that an advanced strand reacted for a relatively short time has a similar normalized strain dependence for  $J_C$  and  $B_{C2}^*(0, 0)$  to advanced strands optimized for high  $J_C$ . Although  $J_C$  is much lower for the PORI strand than the optimized advanced strands in the literature, the  $B_{C2}^*(0, 0)$  values are similar [12]. Reliable comparisons of the (fitting) parameter  $T_C^*(0)$  for different advanced strands are more problem-

atic. Comparing fits to data on different strands, the type of fitting and quantity of data used at high temperature can affect  $T_C^*(0)$ . Equally since the distribution of the critical temperature present (across the compositional variation) in a filament can be large, a measurement of the critical temperature can be strongly dependent on how the measurement is made (e.g. resistive/percolative or magnetic/screening). Fortunately there is detailed thesis work by Naus [34] that suggests the critical temperature only changes by about 0.3 K between 60 h and 300 h in advanced internal-tin strands reacted at 650°C. Hence we conclude that the long heat-treatment's primary effect, from the perspective of the reversible strain properties of  $J_C$ , is to increase the cross-sectional area of superconductor carrying the current without changing the intrinsic critical parameters very significantly and suggest that the normalized strain dependence observed in advanced internal-tin strands can be considered intrinsic to the composition of the  $\text{Nb}_3\text{Sn}$  layer that is produced.

## VI. CONCLUSION

In this paper we have reported comprehensive variable magnetic field, variable temperature and variable strain  $J_C$  data for an advanced internal-tin  $\text{Nb}_3\text{Sn}$  ITER strand (PORI) manufactured by Luvata. The relatively short heat treatment used for the PORI strand leads to significantly lower critical current density than optimized values. However the normalized strain dependence of the critical current at 14 Tesla and 4.2 K is similar to other strands made by an internal-tin process [12]. The parameterization of the data shows that a scaling law can accurately parameterize the  $J_C(B, T, \varepsilon)$  data using just six free parameters. This scaling law is based on assuming a universal behavior of the normalized effective upper critical field for the advanced internal-tin  $\text{Nb}_3\text{Sn}$  strands and provides a framework for comparing partial data sets from different laboratories.

This work shows that the reversible strain dependence of the normalized critical current at 4.2 K and 14 T and the upper critical field [12] are properties intrinsic to advanced internal-tin strands—characteristic of the fabrication route and (beyond 60 h) insensitive to the duration of the heat treatment.

## ACKNOWLEDGMENT

The authors thank the help and support from those in the EFDA and ITER community and in particular members of the Superconductivity Group in Durham including J. Higgins, S. Lishman, and S. Pragnell.

## REFERENCES

- [1] A. Vostner and E. Salpietro, "Enhanced critical current densities in  $\text{Nb}_3\text{Sn}$  superconductors for large magnets," *Supercond. Sci. Technol.*, vol. 19, pp. S90–S95, 2006.
- [2] A. Devred, B. Baudouy, D. E. Baynham, T. Boutboul, S. Canfer, M. Chorowski, P. Fabbriatore, S. Farinon, H. Felice, P. Fessia, J. Fydrich, V. Granata, M. Greco, J. Greenhalgh, D. Leroy, P. Loverige, M. Matkowski, G. Michalski, F. Michel, L. R. Oberli, A. den Ouden, D. Pedrini, S. Pietrowicz, J. Polinski, V. Previtali, L. Quettier, D. Richter, J. M. Rifflet, J. Rochford, F. Rondeaux, S. Sanz, C. Scheuerlein, N. Schwerg, S. Sgobba, M. Sorbi, F. Toral-Fernandez, R. van Weelderden, P. Vedrine, and G. Volpini, "Overview and status of the next european dipole joint research activity," *Supercond. Sci. Technol.*, vol. 19, pp. S67–S83, 2006.

- [3] E. Gregory, M. Tomsic, X. Peng, R. Dhaka, V. R. Nazareth, and M. D. Sumption, "Niobium Tin conductors for high energy physics, fusion, MRI and NMR applications made by different techniques," *IEEE Trans. Appl. Supercond.*, vol. 18, pp. 989–992, 2008.
- [4] D. O. Welch, "Alteration of the superconducting properties of A15 compounds and elementary composite superconductors by nonhydrostatic elastic strain," *Adv. Cryogenic Eng.*, vol. 26, pp. 48–65, 1980.
- [5] A. Godeke, B. ten Haken, and H. H. J. ten Kate, "The deviatoric strain description of the critical properties of Nb<sub>3</sub>Sn conductors," *Physica C*, vol. 372–376, pp. 1295–1298, 2002.
- [6] K. C. Lim, J. D. Thompson, and G. W. Webb, "Electronic density of states and T<sub>C</sub> in Nb<sub>3</sub>Sn under pressure," *Phys. Rev. B*, vol. 27, pp. 2781–2787, 1983.
- [7] D. M. J. Taylor and D. P. Hampshire, "The scaling law for the strain dependence of the critical current density in Nb<sub>3</sub>Sn superconducting wires," *Supercond. Sci. Technol.*, vol. 18, pp. S241–S252, 2005.
- [8] X. F. Lu, S. Pragnell, and D. P. Hampshire, "Small reversible axial-strain window for critical current in both compression and tension for a high performance Nb<sub>3</sub>Sn superconducting strand," *Appl. Phys. Lett.*, vol. 91, p. 132512, 2007.
- [9] A. Godeke, B. ten Haken, H. H. J. ten Kate, and D. Larbalestier, "A general scaling relation for the critical current density in Nb<sub>3</sub>Sn," *Supercond. Sci. Technol.*, vol. 19, pp. R100–R116, 2006.
- [10] S. A. Keys and D. P. Hampshire, "A scaling law for the critical current density of weakly and strongly-coupled superconductors, used to parameterise data from a technological Nb<sub>3</sub>Sn strand," *Supercond. Sci. Technol.*, vol. 16, pp. 1097–1108, 2003.
- [11] S. A. Keys, N. Koizumi, and D. P. Hampshire, "The strain and temperature scaling law for the critical current density of a jelly-roll Nb<sub>3</sub>Al strand in high magnetic fields," *Supercond. Sci. Technol.*, vol. 15, pp. 991–1010, 2002.
- [12] X. F. Lu, D. M. J. Taylor, and D. P. Hampshire, "Critical current scaling laws for advanced Nb<sub>3</sub>Sn superconducting strands for fusion applications with six free parameters," *Supercond. Sci. Technol.*, vol. 21, p. 105016, 2008.
- [13] T. Pyon, J. Somerkoski, H. Kanithi, B. Karlemo, and M. Holm, "Development of high performance Nb<sub>3</sub>Sn conductor for fusion and accelerator applications," *IEEE Trans. Appl. Supercond.*, vol. 17, pp. 2568–2571, 2007.
- [14] C. R. Walters, I. M. Davidson, and G. E. Tuck, "Long sample high sensitivity critical current measurements under strain," *Cryogenics*, vol. 26, pp. 406–412, 1986.
- [15] D. M. J. Taylor and D. P. Hampshire, "Properties of helical springs used to measure the axial strain dependence of the critical current density in superconducting wires," *Supercond. Sci. Technol.*, vol. 18, pp. 356–368, 2005.
- [16] N. Cheggour and D. P. Hampshire, "Unifying the strain and temperature scaling laws for the pinning force density in superconducting niobium-tin multifilamentary wires," *J. Appl. Phys.*, vol. 86, pp. 552–555, 1999.
- [17] N. Cheggour and D. P. Hampshire, "A probe for investigating the effects of temperature, strain, and magnetic field on transport critical currents in superconducting wires and tapes," *Rev. Sci. Instrum.*, vol. 71, pp. 4521–4530, 2000.
- [18] S. A. Keys and D. P. Hampshire, "Characterisation of the transport critical current density for conductor applications," in *Handbook of Superconducting Materials*, D. Cardwell and D. Ginley, Eds. Bristol, U.K.: IOP Publishing, 2003, vol. 2, pp. 1297–1322.
- [19] F. Volker, "Resistance in small, twisted, multicore superconducting wires," *Particle Accelerators*, vol. 1, p. 205, 1970.
- [20] D. M. J. Taylor, S. A. Keys, and D. P. Hampshire, "*E* – *J* characteristics and *n*-values of a niobium-tin superconducting wire as a function of magnetic field, temperature and strain," *Physica C*, vol. 372, pp. 1291–1294, 2002.
- [21] P. Bruzzone, "The index *n* of the voltage-current curve, in the characterization and specification of technical superconductors," *Physica C*, vol. 401, pp. 7–14, 2004.
- [22] D. P. Hampshire and H. Jones, "Critical current of a NbTi reference material as a function of field and temperature," *Magnet Technol.*, vol. 9, pp. 531–535, 1985.
- [23] D. P. Hampshire and H. Jones, "Analysis of the general structure of the *E* – *I* characteristic of high current superconductors with particular reference to a NbTi SRM wire," *Cryogenics*, vol. 27, pp. 608–616, 1987.
- [24] W. H. Warnes and D. C. Larbalestier, "Critical current distributions in superconducting composites," *Cryogenics*, vol. 26, pp. 643–653, 1986.
- [25] T. Luhman, M. Suenaga, and C. J. Klamut, "Influence of tensile stresses on the superconducting temperature of multifilamentary Nb<sub>3</sub>Sn composite conductors," *Adv. Cryogenic Eng.*, vol. 24, pp. 325–330, 1978.
- [26] G. Rupp, "Improvement of critical current of multifilamentary Nb<sub>3</sub>Sn conductors under tensile-stress," *IEEE Trans. Appl. Supercond.*, vol. 13, pp. 1565–1567, 1977.
- [27] W. D. Markiewicz, "Invariant formulation of the strain dependence of the critical temperature T<sub>C</sub> of Nb<sub>3</sub>Sn in a three term approximation," *Cryogenics*, vol. 44, pp. 895–908, 2004.
- [28] W. A. Fietz and W. W. Webb, "Hysteresis in superconducting alloys—Temperature and field dependence of dislocation pinning in niobium alloys," *Phys. Rev.*, vol. 178, pp. 657–667, 1969.
- [29] E. H. Brandt, "Precision Ginzburg-Landau SOLUTION of ideal vortex lattices for any induction and symmetry," *Phys. Rev. Lett.*, vol. 78, pp. 2208–2211, 1997.
- [30] D. Dew-Hughes, "Flux Pinning Mechanisms in Type II Superconductors," *Philos. Mag.*, vol. 30, pp. 293–305, 1974.
- [31] D. M. J. Taylor and D. P. Hampshire, "Relationship between the *n*-value and critical current in Nb<sub>3</sub>Sn superconducting wires exhibiting intrinsic and extrinsic behaviour," *Supercond. Sci. Technol.*, vol. 18, pp. 297–302, 2005.
- [32] J. E. Evetts, J. R. Cave, R. E. Somekh, J. P. Stanton, and A. M. Campbell, "Characterisation of Nb<sub>3</sub>Sn diffusion layer material," *IEEE Trans. Magn.*, vol. 17, pp. 360–363, 1981.
- [33] J. E. Evetts and C. J. G. Plummer, "Flux pinning in polycrystalline A15 bronze route filaments," in *Proc. Int. Symp. on Flux Pinning and Electromagn. Properties of Supercond.*, Fukuoka, Japan, 1985, pp. 146–151.
- [34] M. T. Naus, "Optimization of Internal-Sn Nb<sub>3</sub>Sn Composites," Thesis, Univ. Wisconsin, Madison, 2002.